



HAL
open science

Investigation of the Diamagnetic Drift Condition for the Suppression of Magnetic Reconnection in 3D Interlinked Reconnection Events with Magnetic Flux Pileup

K. Maheshwari, T. D. Phan, M. Øieroset, N. Fargette, B. Lavraud, J. L. Burch, R. J. Strangeway, D. J. Gershman, B. L. Giles

► **To cite this version:**

K. Maheshwari, T. D. Phan, M. Øieroset, N. Fargette, B. Lavraud, et al.. Investigation of the Diamagnetic Drift Condition for the Suppression of Magnetic Reconnection in 3D Interlinked Reconnection Events with Magnetic Flux Pileup. *The Astrophysical Journal*, 2022, 940, 10.3847/1538-4357/ac9405 . insu-04472241

HAL Id: insu-04472241

<https://insu.hal.science/insu-04472241>

Submitted on 23 Feb 2024

HAL is a multi-disciplinary open access archive for the deposit and dissemination of scientific research documents, whether they are published or not. The documents may come from teaching and research institutions in France or abroad, or from public or private research centers.

L'archive ouverte pluridisciplinaire **HAL**, est destinée au dépôt et à la diffusion de documents scientifiques de niveau recherche, publiés ou non, émanant des établissements d'enseignement et de recherche français ou étrangers, des laboratoires publics ou privés.



Distributed under a Creative Commons Attribution 4.0 International License



Investigation of the Diamagnetic Drift Condition for the Suppression of Magnetic Reconnection in 3D Interlinked Reconnection Events with Magnetic Flux Pileup

K. Maheshwari^{1,7} , T. D. Phan¹ , M. Øieroset¹ , N. Fargette² , B. Lavraud^{2,3} , J. L. Burch⁴ , R. J. Strangeway⁵ ,
D. J. Gershman⁶ , and B. L. Giles⁶

¹ Space Sciences Laboratory, University of California, Berkeley, CA 94720, USA; kmaheshwari@princeton.edu

² IRAP, CNRS, CNES, Université de Toulouse, Toulouse, France

³ Laboratoire d'astrophysique de Bordeaux, Université de Bordeaux, CNRS, Pessac, France

⁴ Southwest Research Institute, San Antonio, TX 78238, USA

⁵ University of California, Los Angeles, CA 90095, USA

⁶ NASA Goddard Space Flight Center, Greenbelt, MD 20771, USA

Received 2022 August 17; revised 2022 September 13; accepted 2022 September 20; published 2022 December 2

Abstract

We have performed a statistical survey to investigate possible diamagnetic drift suppression of magnetic reconnection using Magnetospheric Multiscale observations of interlinked magnetic field line events at Earth's magnetopause. Our goal is to investigate a possible cause for the observed magnetic field pileup on the two sides of the thin reconnecting current sheets, at the interface of the converging field lines. We compare whether the diamagnetic drift condition for the suppression of reconnection is satisfied before and after magnetic field pileup. We find that for a majority of events in our data set, the pre-pileup plasma β gradient and magnetic shear values were in the reconnection-suppressed regime, whereas the post-pileup values were in the reconnection-allowed regime. A possible interpretation is that reconnection was suppressed under the pre-pileup conditions, and this led to magnetic field pileup. The magnetic field pileup subsequently generated boundary conditions at the interlinked current sheet that overcame the diamagnetic drift suppression condition, allowing reconnection to happen in the interlinked field line structure. However, in one third of the events, the pre-pileup conditions were already in the reconnection-allowed regime, indicating that in such events, the diamagnetic suppression condition was probably not responsible for field pileup.

Unified Astronomy Thesaurus concepts: [Geomagnetic fields \(646\)](#); [Solar magnetic reconnection \(1504\)](#)

1. Introduction

Magnetic reconnection in current sheets is a universal plasma process that converts magnetic energy into plasma jetting and heating and is important in many laboratory, space, solar, and astrophysical contexts (Yamada 2010; Paschmann et al. 2013). In situ observations have revealed the occurrence of reconnection at Earth's magnetopause and magnetotail, in the magnetosheath, as well as in the solar wind (see review paper by Paschmann et al. 2013).

Recently, a new 3D reconnection phenomenon was discovered at Earth's magnetopause in which reconnection occurs at the interface of converging field lines as the approaching field lines get tangled up (Øieroset et al. 2016; Kacem et al. 2018; Øieroset et al. 2019; Fargette et al. 2020; Qi et al. 2020; Russell & Qi 2020). The converging field lines are thought to originate from two active reconnection X-lines. A particular characteristic of these events is the presence of significant magnetic flux pileup in the two inflow regions leading up to the interface current sheet. Recently, similar field pileup reconnection events have been reported in some solar wind current sheets (Fargette et al. 2021). Such flux pileup reconnection is rarely seen in standard reconnection events observed at the magnetopause, in the magnetotail, magnetosheath, or the solar wind. Thus, the interlinked field line events provide a

unique opportunity to study reconnection in the magnetic flux pileup regime. One fundamental question is why the magnetic field piles up in interlinked reconnection.

Øieroset et al. (2019) studied three interlinked reconnection events in detail and found that for all three events the field pileup was associated with a decrease in plasma $\Delta\beta$ and an increase in magnetic shear across the reconnecting current sheet, where β is the ratio of plasma pressure to magnetic pressure. Swisdak et al. (2003, 2010) predicted that the occurrence of reconnection in a current sheet depends on the difference in the β on the two sides of the current sheet, as well as the magnetic shear angle, θ , across the current sheet. The underlying physics is related to the diamagnetic drift of the X-line associated with the plasma pressure gradient across the current sheet. Reconnection is deemed to be suppressed if the X-line drift speed along the reconnection outflow direction exceeds the reconnection outflow speed. For a given θ , reconnection is suppressed if $\Delta\beta$ satisfies the following equation:

$$\Delta\beta > 2(L/d_i) \tan(\theta/2) \quad (1)$$

where L/d_i is the width of the plasma pressure gradient layer across the current sheet (near the X-line) in units of the ion skin depth d_i . This width is expected to be related to the width of the diffusion region, which is on the order of one d_i .

Thus, the Øieroset et al. (2019) case studies suggest that the magnetic field pileup may have been necessary to overcome the diamagnetic suppression condition for reconnection (1). If confirmed, this interpretation would have important implications for the understanding of 3D interactions of entangled field lines; a scenario that should commonly occur in multiple X-line

⁷ Currently at Princeton University/Princeton Plasma Physics Laboratory.



reconnection in the presence of finite guide magnetic fields (Fargette et al. 2020).

In this paper, we report the findings of a statistical study of the diamagnetic drift suppression condition (1) as applied to interlinked (field pileup) reconnection events at Earth’s magnetopause, using a database of 43 such events initially reported by Fargette et al. (2020). In the Fargette et al. study, it was found that for most of the events, the $\Delta\beta$ and θ conditions immediately adjacent to the current sheet were in the regime where reconnection is not predicted to be suppressed. In the present study, we expand the Fargette et al. study by examining, in addition, the $\Delta\beta$ and θ conditions in the two inflow regions further upstream of the interlinked current sheet, where the magnetic field pileup begins on both sides of the current sheet. By comparing the conditions prior to magnetic flux pileup with the conditions immediately adjacent to the interface current sheet, our study sheds light on how boundary conditions may evolve to trigger reconnection in situations where the initial conditions may not be favorable for reconnection.

The paper is organized as follows: In Section 2 we discuss the database and instrumentation. Section 3 describes the coordinate system used. In Section 4 we show individual examples of interlinked events to illustrate how the pre- and post-pileup times are determined. We describe the findings of the statistical study in Section 5. Section 6 discusses the implications for the cause of field pileup in interlinked reconnection events.

2. Database of Interlinked Reconnection Events

We use a data set of 43 interlinked reconnection events observed by the Magnetospheric Multiscale (MMS) mission previously compiled by Fargette et al. (2020). The events were identified based on the presence of (1) enhanced magnetic pressure toward the center of the event, (2) a sharp current sheet at the center of the event near the peak of magnetic pressure, and (3) reconnection signatures inside the current sheet. Three examples will be shown in Section 4 to illustrate our methodology for identifying in the data the pre- and post-pileup conditions.

We use burst-mode magnetic field data from the fluxgate magnetometer at 128 samples per second (Russell et al. 2014), and plasma data from the Fast Plasma Investigation (FPI) instruments at 150 ms resolution for ions and 30 ms for electrons (Pollock et al. 2016). The data shown in the study are from the MMS1 spacecraft.

3. Current Sheet Coordinate System

Although it is possible to deduce the presence or absence of reconnection jets in any coordinate system, the signature of a reconnection jet is clearest when the data is displayed in the current sheet LMN coordinate system, with L along the reconnecting field (or outflow) direction, M along the X-line, and N along the current sheet normal. Because most events in our data set have low magnetic shear (large guide field) current sheets, we use a hybrid variance analysis method to determine the current sheet coordinate system (Gosling & Phan 2013), which has been found to work well for such current sheets. The current sheet normal direction, N , is determined from $\mathbf{B}_1 \times \mathbf{B}_2 / |\mathbf{B}_1 \times \mathbf{B}_2|$, where \mathbf{B}_1 and \mathbf{B}_2 are the magnetic field vectors at the two edges of the current sheet; $\mathbf{M} = \mathbf{N} \times \mathbf{L}'$,

where L' is the direction of the maximum variance of the magnetic field (Sonnerup & Cahill 1967); $\mathbf{L} = \mathbf{M} \times \mathbf{N}$ completes the coordinate system.

4. Examples of Interlinked Reconnection Events

In this section we describe three examples of interlinked reconnection events from the Fargette et al. (2020) data set. These events help illustrate our methodology for selecting the pre- and post-pileup times for the statistical study. They also serve to illustrate the challenges. The first example (Section 4.1) shows clear, nearly monotonic pileup of the reconnecting component of the magnetic field. In this case, the pre-pileup times can be taken simply as the times where the pileup starts, and the post-pileup times can be taken where the pileup ends, i.e., at the edges of the current sheet. The next two examples (Section 4.2) illustrate events that show nonmonotonic field pileup, which makes the determination of the pre-pileup times more challenging.

4.1. Clear Magnetic Field Pileup Example

Figure 1 shows a magnetic field structure between the two vertical blue dashed lines, with field strength enhancement toward the center of the event from both sides (Figure 1(a)) and a sharp reversal of the antiparallel component of the magnetic field, B_L (Figure 1(b)). The abrupt B_L reversal at the center of the $|\mathbf{B}|$ pileup, together with the different electron pitch angle flux characteristics across the field reversal (Figure 1(f)), indicates the presence of a thin current sheet that separates two plasmas that are not magnetically connected with each other, instead of a standard magnetic flux rope (Kacem et al. 2018; Øieroset et al. 2019; Fargette et al. 2020). Within the current sheet, between the two vertical red dashed lines, there is an ion jet in $V_{L,i}$ (Figure 1(c)). These characteristics are similar to those previously observed and interpreted as reconnection at the interface of interlinked field lines originating from multiple reconnection sites at the magnetopause (see Figure 1(g); Øieroset et al. 2016; Kacem et al. 2018; Øieroset et al. 2019; Fargette et al. 2020; Russell & Qi 2020).

In addition to the $|\mathbf{B}|$ pileup, the reconnecting field component, $|B_L|$, shows a steady increase toward the current sheet from both sides, indicating flux pileup. The goal of the present study is to investigate the possible cause of the magnetic flux pileup in relation to the $\Delta\beta$ - θ condition (1) (Swisdak et al. 2010). Thus, we determine $\Delta\beta$ and θ before and after field pileup as one approaches the current sheet from both sides. The two vertical blue lines mark the beginning of the $|B_L|$ field pileup, and the red lines mark the edges of the thin current sheet, which correspond to the end of the field pileup. In this study, we make the assumption (or hypothesis) that the beginning of the pileup (on both sides of the current sheet) corresponds to the state of the current sheet prior to the pileup; $\Delta\beta$ and θ for the pre- (post-) pileup conditions are the difference in β and the relative angle between the magnetic fields at the two blue (red) lines, respectively. As is common in most clear pileup events, the pre-pileup times in this event correspond to local minima in $|\mathbf{B}|$. For this event, the pre-pileup $\Delta\beta$ and θ were, respectively, 2.65 and 10°, while the post-pileup values were 0.36 and 81°. Thus, for this event (event 13 in Table 1 and in Figures 3(b) and (c)), the pre-pileup values (blue data points in Figures 3(a) and (b)) were in the reconnection-suppression regime (below the Equation (1)

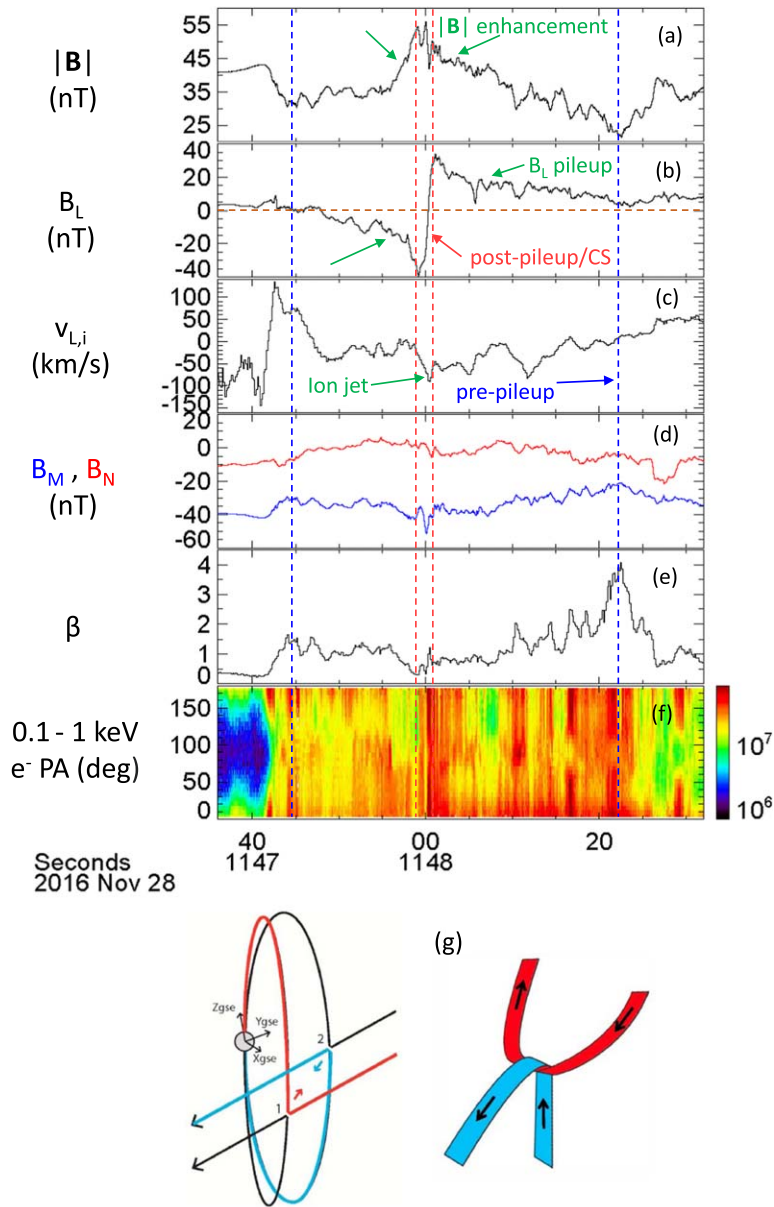


Figure 1. MMS1 observations in LMN of an interface current sheet associated with clear, monotonic pileup in B_L and $|\mathbf{B}|$. Blue vertical lines indicate the chosen pre-pileup locations, and red vertical lines indicate the current sheet edges (i.e., and post-pileup locations). (a) Magnetic field magnitude, (b) reconnecting B_L magnetic field component, (c) ion velocity, (d) B_M and B_N magnetic field components, (e) plasma β , (f) electron pitch angle distribution, and (g) sketch showing interlinked reconnection as a result of colliding field lines emanating from two X-lines at the magnetopause (adapted from Øieroset et al. 2019). This event corresponds to event 13 in Table 1.

curve), whereas the post-pileup values (in red) were in the reconnection-allowed regime (above the curve).

4.2. Complex Field Structure Examples

Figures 2(a)–(f) show an example of more complex field structures around an interlinked current sheet in the Fargette et al. (2020) data set (event 12 in Table 2 and in Figures 3(e) and (f)). The event shows the presence of a current sheet (between the two red vertical lines) with large B_L reversal (Figure 2(b)) near the peak of a $|\mathbf{B}|$ increase (Figure 2(a)). An ion jet is seen inside the current sheet (Figure 2(c)), consistent with reconnection. The electron pitch angle characteristics were different on the two sides of the current sheet (Figure 2(f)), indicating that the plasmas on the two sides were not magnetically connected, consistent with the interlinked field

line interpretation (Kacem et al. 2018). In this example, the B_L pileup was nonmonotonic and jagged on both sides of the current sheet. Thus, while the post-pileup times that correspond to the two edges of the current sheet are well defined, the pre-pileup times are more ambiguous. In order to maintain consistency with other events, we picked the pre-pileup times to be at local minima in $|\mathbf{B}|$ that typically bound the $|\mathbf{B}|$ increase, although it is recognized that there is significant ambiguity in the pre-pileup times in such a nonmonotonic event. For this event, the pre-pileup $\Delta\beta$ and θ were 52.83 and 86°, respectively, placing them in the reconnection-suppressed zone, while the post-pileup values were 1.21 and 53°, very close to the marginal state of condition (1).

Figures 2(g)–(l) show another example of not well-defined pre-pileup conditions around an interlinked current sheet (event

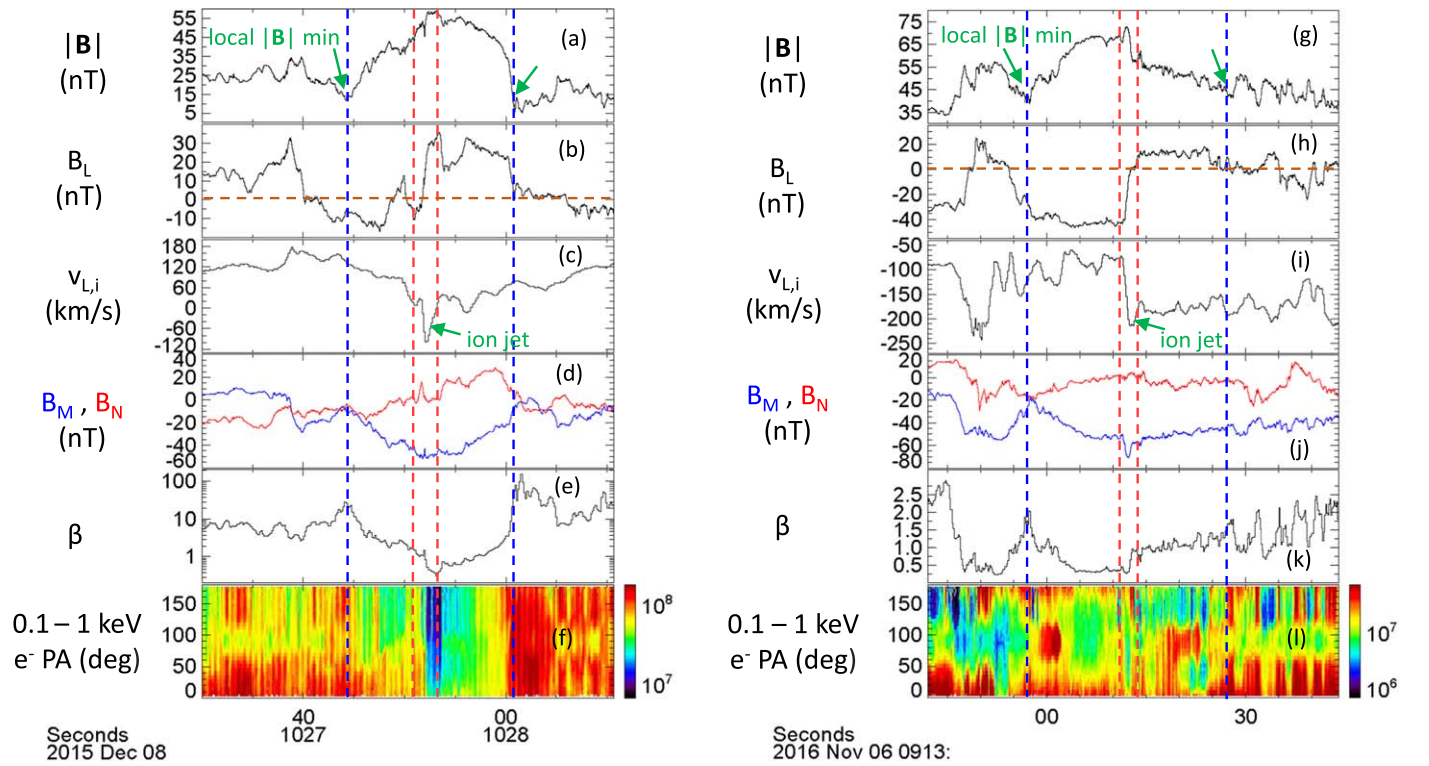


Figure 2. MMS1 observations in LMN of two interface current sheets with nonmonotonic pileup. Blue and red vertical lines indicate the chosen pre- and post-pileup locations, respectively. For each time series, the panels indicate (a), (g) magnetic field magnitude; (b), (h) reconnecting B_L magnetic field component; (c), (i) ion velocity; (d), (j) B_M and B_N magnetic field components; (e), (k) plasma β ; and (f), (l) electron pitch angle distribution. The left (right) column event corresponds to event 12 (19) in Table 2.

19 in Table 2 and in Figures 3(e) and (f). In this event, a reconnecting current sheet was observed near the peak of $|\mathbf{B}|$ enhancement (Figure 2(g)), recognized by a sharp reversal in B_L (Figure 2(h)) and the presence of an embedded ion jet (Figure 2(i)). While the post-pileup times (i.e., the two edges of the current sheet) are well defined, it is more difficult to pinpoint the pre-pileup locations because B_L was steady for ~ 15 s adjacent to the current sheet on both sides, with sudden and variable changes in B_L further away. For consistency, we again picked the locations of local $|\mathbf{B}|$ minima flanking the enhanced $|\mathbf{B}|$ structure as the pre-pileup locations. The occurrence of such $|\mathbf{B}|$ minima bounding a $|\mathbf{B}|$ enhancement structure is a characteristic that is common among most ($>70\%$) of the interlinked reconnection events.

For this event, the pre-pileup $\Delta\beta$ and θ were 0.35 and 56° , placing them in the reconnection-allowed zone already before pileup. The post-pileup values were 0.14 and 53° , thus also in the reconnection-allowed zone.

The two complex structure events described in this section illustrate the difficulty with assigning error bars to the estimated pre-pileup $\Delta\beta$ and θ values in a meaningful way. This is because the biggest errors are not associated with the variability of β and the magnetic field around well-defined pre-pileup locations. Rather, they are due mainly to the uncertain pre-pileup locations of the events, which makes the errors challenging to quantify accurately by error bars. For this reason, no error estimates on $\Delta\beta$ and θ will be shown in the statistical results presented in the next section. The errors on the post-pileup $\Delta\beta$ and θ conditions are expected to be small because the locations of the current sheet edges are usually well defined.

5. Statistical Survey of Pre- and Post-pileup Conditions of Interlinked Reconnection

Of the 43 interlinked reconnection events reported by Fargette et al. (2020), we identified a subset of 18 events displaying nearly monotonic field pileup similar to the event discussed in Section 4.1 and shown in Figure 1. This type of event shows clear enhancements in $|\mathbf{B}|$ and an intense current sheet near the peak of $|\mathbf{B}|$, monotonic increase of $|B_L|$ on both sides of the current sheet, reconnecting signatures inside the current sheet, and differing electron pitch angle distributions on the two sides of the current sheet.

For these 18 clear (monotonic) events, the two edges of the current sheet are well defined and mark the post-pileup locations. Our independently determined current sheet edges are generally close to those reported by Fargette et al. (2020).

To estimate the pre-pileup locations, we worked outwards from the current sheet, using a combination of following the decrease of $|B_L|$ until the decrease stopped, as well as following $|\mathbf{B}|$ until a local minimum was reached (as in Figure 1).

The other 25 events in the Fargette et al. database are characterized by a nonmonotonic pileup in B_L . In these cases, determining the pre-pileup times is challenging and therefore more subjective. Two such examples were described in Section 4.2. The nonmonotonic pileup events are difficult to classify into specific categories of behavior because there is a large variety of behavior. For consistency with the methodology for the clear pileup events, we generally set the pre-pileup times to be at local $|\mathbf{B}|$ minima that bound the enhanced $|\mathbf{B}|$ structures (e.g., Figures 2(a) and (f)). Such minima could be identified in 18 of the 25 nonmonotonic events, but the

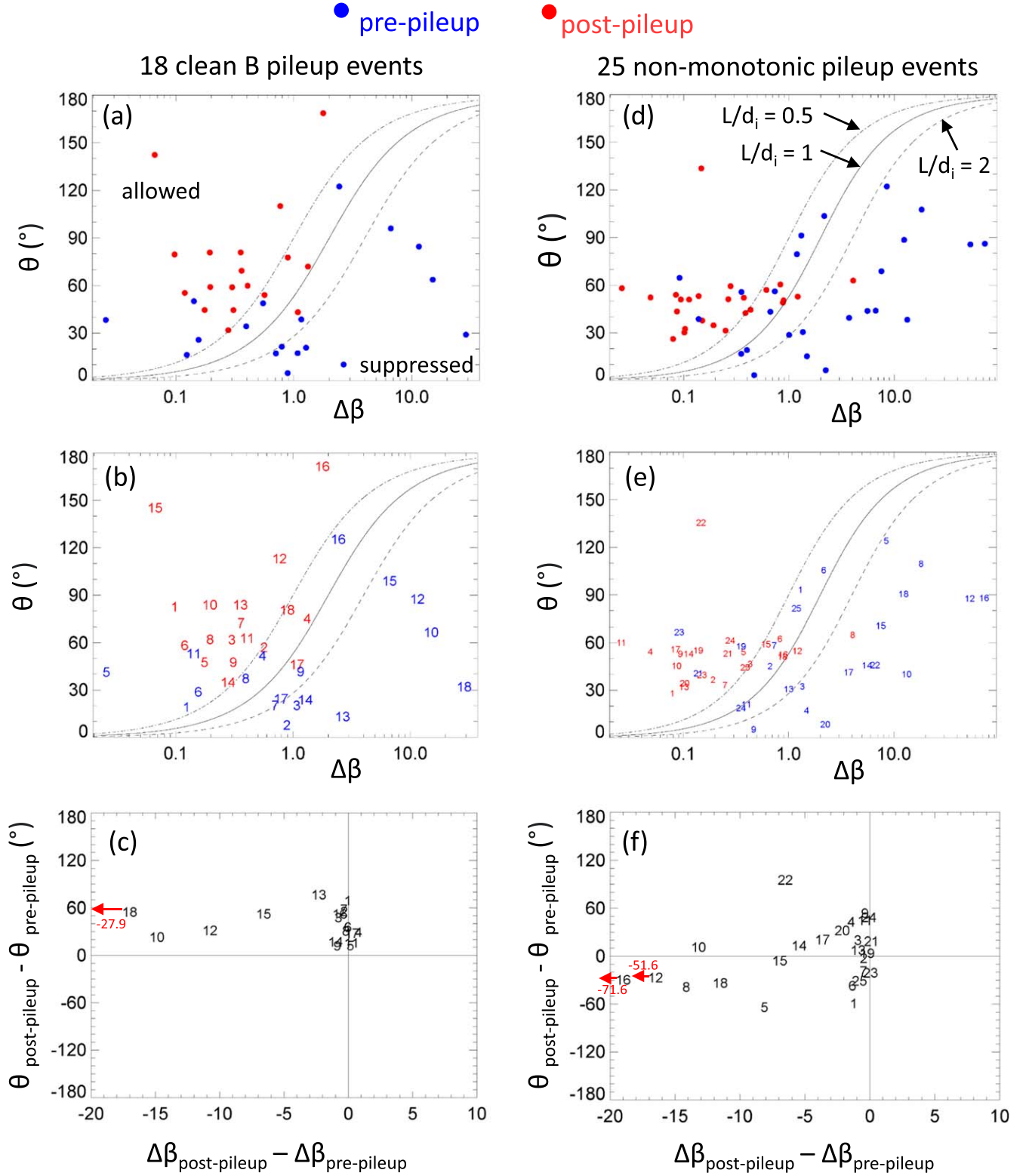


Figure 3. Statistics on 18 monotonic pileup events (left panels) and 25 nonmonotonic pileup events (right panels). ((a) and (d)) Magnetic shear vs. $\Delta\beta$ with pre-pileup in blue and post-pileup in red. ((b) and (e)) Same as (a) and (d) but with event numbers corresponding to Tables 1 and 2 indicated. ((c) and (f)) Change in the magnetic shear and the change in the $\Delta\beta$ over the course of the pileup. The three curves in panels (a), (b), (d), and (e) are the theoretical curves (Equation (1)) for three values of the density gradient scale at the X-line, in units of the ion inertial length d_i (Swisdak et al. 2010). The theory predicts the suppression of reconnection below these curves.

remaining events (events 7, 13, 14, 16, 21, 24, and 25 in Table 2) do not show well-defined $|\mathbf{B}|$ minima or the $|\mathbf{B}|$ minima clearly do not represent the beginning of field pileup. In the latter events, the selection of the pre-pileup times is more

subjective. Because of these challenges, the findings from the 25 nonmonotonic events are generally less reliable than those from the 18 clear pileup events. We will therefore discuss the two subsets of events separately.

5.1. Subset of 18 Nearly Monotonic B_L Pileup Events

Figure 3(a) shows the $\Delta\beta$ and magnetic shear θ parameters before (blue) and after (red) pileup for the 18 clear pileup event subset, listed in Table 1. Overlaid is the theoretical boundary between the reconnection-suppressed and reconnection-allowed regimes according to Equation (1), for $L/d_i = 0.5, 1,$ and 2 . Below, we will discuss our findings in relation to the choice of $L/d_i = 1$, as suggested by the theoretical expectation of the reconnection diffusion region width and supported by some previous experimental studies (e.g., Phan et al. 2010, 2013). Figure 3(b) shows the same events as in Figure 3(a), but with event numbers (corresponding to Table 1) labeled. Figure 3(c) shows the difference in magnetic shear before and after pileup for each event versus the corresponding difference in $\Delta\beta$. Figures 3(b) and (c) allow tracking of the evolution of $\Delta\beta$ and θ of the individual events from their pre- to post-pileup states.

Two main findings stand out:

1. After pileup (red data points) most events (17/18) were in the reconnection-allowed zone, i.e., with $\Delta\beta < 2 \tan(\theta/2)$, while before pileup (blue data points) 11 out of 18 events were in the reconnection-suppressed zone (Figure 3(a)).
2. For a large majority of the events (14/18), $\Delta\beta$ decreased and the magnetic shear θ increased from pre-pileup to post-pileup (Figures 3(b) and (c)).

Interestingly, in seven of the events the pre-pileup $\Delta\beta$ and θ values were already in the reconnection-allowed regime. Thus, the diamagnetic drift suppression of reconnection condition was likely not responsible for the magnetic field pileup in those events. While three of the seven cases did not result in a decrease of $\Delta\beta$ post-pileup compared to pre-pileup, all seven events remained in the reconnection-allowed zone post-pileup. Detailed investigations of the three events reveal that the pre-pileup plasma β was already low (< 0.6), which contributed to the low pre-pileup $\Delta\beta$.

For the 11 events where the pre-pileup was in the suppression zone, 10 events underwent an increase in magnetic shear angle θ and decrease in $\Delta\beta$, with those same 10 events ending up in the reconnection-allowed zone post-pileup. This is a nontrivial finding, because while $|\mathbf{B}|$ pileup usually leads to reduced β , therefore increasing the likelihood for a reduced $\Delta\beta$ as well, there is no a priori reason why the pre- and post-pileup conditions should be on opposite sides of the marginal $\Delta\beta = 2 \tan(\theta/2)$ curve.

Furthermore, all 18 events show an increase in magnetic shear angle θ going from pre-pileup to post-pileup (see Figure 3(c)). This is not a trivial finding because there is usually a $|B_M|$ enhancement together with a $|B_L|$ enhancement on approach to the interlinked current sheets in both inflow regions (see Figures 1(d), 2(d), and 2(j)), which could in principle not lead to an increase in θ .

5.2. Subset of 25 Nonmonotonic B_L Pileup Events

We now examine the subset of 25 events, listed in Table 2, that had nonmonotonic field pileup, which made the pre-pileup times difficult to determine. Figures 3(d) and (e) show that most of the post-pileup $\Delta\beta$ and θ values were in the reconnection-allowed zone, with only two events having the post-pileup conditions in the reconnection-suppressed zone. On

the other hand, while two thirds of the events (17 of the 25) were in the reconnection-suppressed zone before pileup, one third (eight events) were already in the reconnection-allowed zone pre-pileup. These statistics are surprisingly similar to the 18 clean pileup events (Section 5.1).

Figure 3(f) shows that for most events, $\Delta\beta$ decreased from pre- to post-pileup (with most points being in the left quadrants) due to the increase in $|\mathbf{B}|$ and decrease of β in interlinked reconnection events. However, unlike the 18 clear pileup events that showed increasing magnetic shear associated with field pileup in all events, approximately half of the 25 nonmonotonic pileup events showed a decrease in magnetic shear instead.

6. Summary and Discussion

We have studied a possible cause for the magnetic field pileup associated with interlinked reconnection at Earth's magnetopause. Magnetic field pileup in the inflow regions is rarely seen in standard reconnection events observed in space, but it is a striking feature in interlinked reconnection events. A possible reason for field pileup on approach to a current sheet could be a lack of reconnection in the current sheet. Magnetic flux pileup against a nonreconnecting current sheet has been observed at Earth's low-latitude magnetopause during northward interplanetary magnetic field conditions, when the magnetosheath field is parallel to the geomagnetic field and there is no (or less effective) reconnection (e.g., Paschmann et al. 1993; Phan et al. 1994).

In this paper, we study the phenomenon of interlinked field lines at the magnetopause. In 3D, field lines originating from multiple X-lines can become interlinked when they meet (Øieroset et al. 2016; Kacem et al. 2018; Øieroset et al. 2019; Fargette et al. 2020; Russell & Qi 2020). If reconnection occurs readily and is sufficiently fast as the field lines meet, there would be no magnetic field pileup. The hypothesis we examined in this study is whether the $\Delta\beta$ and θ conditions are not favorable for reconnection to occur when the field lines first meet, leading to the field pileup and magnetic shear increase, which eventually overcome the diamagnetic drift suppression condition. This hypothesis was first raised by Øieroset et al. (2019) in a case study based on three interlinked reconnection events. The purpose of the present study is to test this hypothesis using a larger database of interlinked reconnection events.

We have analyzed the Fargette et al. (2020) data set of reconnecting current sheets at the interface of interlinked field lines to investigate if flux pileup in the inflow regions of these events may be related to the Swisdak et al. (2003, 2010) diamagnetic drift suppression condition. First, we determined where in the data the flux pileup occurred. For a subset of 18 events, the pileup of the reconnecting field component (B_L) was nearly monotonic, and the location of the start of the B_L pileup in both inflow regions could be unambiguously identified. For the other 25 events in the data set, the pileup was not monotonic, and thus determining where to mark the start of the field pileup was challenging. In these cases, the pre-pileup locations (or times) were taken at local minima of $|\mathbf{B}|$ that flanked the field pileup structure, although in some events, there were no clear $|\mathbf{B}|$ minima or the $|\mathbf{B}|$ minima clearly did not correspond to the start of the B_L pileup. Thus, this subset of 25 events is associated with ambiguities in determining the pre-pileup parameters.

Table 1
18 Monotonic Flux Pileup Events

Event	Current Sheet Left	Current Sheet Right	Pre-pileup Left	Pre-pileup Right
1	2015-09-10/ 19:58:30.029	2015-09-10/ 19:58:31.259	2015-09-10/ 19:58:26.710	2015-09-10/ 19:58:33.630
2	2015-09-10/ 20:32:02.518	2015-09-10/ 20:32:04.140	2015-09-10/ 20:31:55.180	2015-09-10/ 20:32:16.430
3	2015-09-15/ 15:32:27.910	2015-09-15/ 15:32:29.720	2015-09-15/ 15:32:20.750	2015-09-15/ 15:32:40.789
4	2015-10-20/ 14:45:43.029	2015-10-20/ 14:45:45.450	2015-10-20/ 14:45:36.900	2015-10-20/ 14:45:48.599
5	2015-10-22/ 13:37:16.269	2015-10-22/ 13:37:19.609	2015-10-22/ 13:37:03.500	2015-10-22/ 13:37:29.680
6	2015-10-31/ 07:18:35.776	2015-10-31/ 07:18:39.610	2015-10-31/ 07:18:04.099	2015-10-31/ 07:19:07.000
7	2015-11-07/ 14:16:39.500	2015-11-07/ 14:16:41.599	2015-11-07/ 14:16:21.299	2015-11-07/ 14:17:05.700
8	2015-11-21/ 01:56:48.000	2015-11-21/ 01:56:52.993	2015-11-21/ 01:56:03.799	2015-11-21/ 01:57:20.299
9	2015-12-05/ 23:45:45.577	2015-12-05/ 23:45:50.750	2015-12-05/ 23:45:30.299	2015-12-05/ 23:46:02.299
10	2016-02-03/ 05:37:43.922	2016-02-03/ 05:37:49.315	2016-02-03/ 05:37:27.500	2016-02-03/ 05:38:01.700
11	2016-02-28/ 01:17:52.031	2016-02-28/ 01:17:53.359	2016-02-28/ 01:17:47.049	2016-02-28/ 01:17:56.970
12	2016-10-06/ 17:30:26.589	2016-10-06/ 17:30:32.119	2016-10-06/ 17:30:21.440	2016-10-06/ 17:30:42.569
13	2016-11-28/ 11:47:59.100	2016-11-28/ 11:48:01.066	2016-11-28/ 11:47:44.799	2016-11-28/ 11:48:22.500
14	2016-12-10/ 04:53:31.299	2016-12-10/ 04:53:36.000	2016-12-10/ 04:53:04.000	2016-12-10/ 04:54:07.000
15	2016-12-26/ 13:41:14.450	2016-12-26/ 13:41:19.170	2016-12-26/ 13:40:48.660	2016-12-26/ 13:41:37.849
16	2016-12-27/ 10:16:41.839	2016-12-27/ 10:16:44.200	2016-12-27/ 10:16:29.809	2016-12-27/ 10:16:57.160
17	2016-12-28/ 05:01:30.509	2016-12-28/ 05:01:32.660	2016-12-28/ 05:01:06.599	2016-12-28/ 05:01:49.700
18	2017-01-01/ 02:14:40.309	2017-01-01/ 02:14:40.935	2017-01-01/ 02:14:38.660	2017-01-01/ 02:14:43.599

Table 2
25 Nonmonotonic Flux Pileup Events

Event	Current Sheet Left	Current Sheet Right	Pre-pileup Left	Pre-pileup Right
1	2015-09-15/ 15:48:12.597	2015-09-15/ 15:48:14.372	2015-09-15/ 15:48:04.000	2015-09-15/ 15:48:17.100
2	2015-10-11/ 10:50:40.500	2015-10-11/ 10:50:45.600	2015-10-11/ 10:50:30.099	2015-10-11/ 10:51:00.900
3	2015-10-11/ 12:49:13.019	2015-10-11/ 12:49:16.084	2015-10-11/ 12:49:04.829	2015-10-11/ 12:49:26.289
4	2015-10-13/ 06:01:58.630	2015-10-13/ 06:02:09.200	2015-10-13/ 06:01:30.900	2015-10-13/ 06:02:24.000
5	2015-10-14/ 08:57:21.000	2015-10-14/ 08:57:26.324	2015-10-14/ 08:56:18.000	2015-10-14/ 08:57:50.000
6	2015-10-17/ 12:22:52.892	2015-10-17/ 12:22:57.120	2015-10-17/ 12:22:30.599	2015-10-17/ 12:23:02.099
7	2015-10-17/ 12:33:02.099	2015-10-17/ 12:33:07.395	2015-10-17/ 12:32:28.200	2015-10-17/ 12:33:23.299
8	2015-10-22/ 13:27:48.764	2015-10-22/ 13:27:54.865	2015-10-22/ 13:27:20.000	2015-10-22/ 13:28:00.299
9	2015-10-22/ 13:39:29.932	2015-10-22/ 13:39:31.900	2015-10-22/ 13:39:06.599	2015-10-22/ 13:40:04.200
10	2015-11-05/ 14:47:20.437	2015-11-05/ 14:47:21.839	2015-11-05/ 14:47:03.299	2015-11-05/ 14:47:32.299
11	2015-12-02/ 10:07:10.599	2015-12-02/ 10:07:19.700	2015-12-02/ 10:07:00.700	2015-12-02/ 10:07:35.200
12	2015-12-08/ 10:27:51.000	2015-12-08/ 10:27:53.369	2015-12-08/ 10:27:44.400	2015-12-08/ 10:28:00.849
13	2016-02-04/ 03:12:08.410	2016-02-04/ 03:12:12.038	2016-02-04/ 03:11:49.440	2016-02-04/ 03:12:21.029
14	2016-02-06/ 21:00:29.440	2016-02-06/ 21:00:32.650	2016-02-06/ 20:59:23.500	2016-02-06/ 21:01:00.900
15	2016-02-10/ 02:47:51.500	2016-02-10/ 02:47:56.700	2016-02-10/ 02:47:26.099	2016-02-10/ 02:48:10.900
16	2016-02-22/ 23:12:05.567	2016-02-22/ 23:12:06.894	2016-02-22/ 23:12:01.869	2016-02-22/ 23:12:15.740
17	2016-02-26/ 01:49:00.689	2016-02-26/ 01:49:01.376	2016-02-26/ 01:48:58.049	2016-02-26/ 01:49:04.980
18	2016-03-01/ 01:10:23.099	2016-03-01/ 01:10:27.799	2016-03-01/ 01:09:56.509	2016-03-01/ 01:11:10.799
19	2016-11-06/ 09:13:11.349	2016-11-06/ 09:13:14.089	2016-11-06/ 09:12:57.359	2016-11-06/ 09:13:27.549
20	2016-11-12/ 17:50:46.036	2016-11-12/ 17:50:47.683	2016-11-12/ 17:50:31.569	2016-11-12/ 17:51:15.279
21	2016-11-28/ 11:33:15.890	2016-11-28/ 11:33:18.564	2016-11-28/ 11:32:57.869	2016-11-28/ 11:33:28.559
22	2016-12-26/ 10:17:50.950	2016-12-26/ 10:17:53.583	2016-12-26/ 10:17:46.769	2016-12-26/ 10:17:57.660
23	2016-12-28/ 04:59:34.299	2016-12-28/ 04:59:35.000	2016-12-28/ 04:59:10.190	2016-12-28/ 04:59:54.720
24	2017-01-24/ 02:24:30.240	2017-01-24/ 02:24:33.015	2017-01-24/ 02:24:17.000	2017-01-24/ 02:24:43.000
25	2017-01-26/ 01:22:53.084	2017-01-26/ 01:22:55.860	2017-01-26/ 01:22:46.900	2017-01-26/ 01:23:01.700

Since the goal of the present study is to investigate whether the pileup of the reconnecting field component, B_L , is related to the diamagnetic suppression condition or not, for which accurate and reliable measurements of the pre-pileup conditions are required, we now focus the discussion on the findings from the 18 clean B_L pileup events. Comparing the pre- and post-pileup $\Delta\beta$ and θ , we found that of the 11 events that started out in the reconnection-suppressed regime before pileup, 10 moved into the reconnection-allowed regime as pileup occurred. Although the decrease in $\Delta\beta$ associated with $|B|$ pileup is

somewhat expected because β itself decreases with increasing $|B|$, there is no a priori reason why the pre- and post-pileup conditions would be on opposite sides of the marginal $\Delta\beta = 2 \tan(\theta/2)$ curve. Thus, this finding suggests that when field lines from multiple X-lines approach each other, the initial $\Delta\beta$ and θ conditions could be in the regime where reconnection is suppressed. The lack of reconnection causes B_L pileup, leading to decreasing $\Delta\beta$ and increasing magnetic shear, which eventually overcome the diamagnetic drift suppression condition, allowing reconnection to happen.

If the above scenario is correct, and the diamagnetic drift suppression condition is the main reason for the field pileup, we have identified two potential puzzles requiring resolution:

(1) One would expect the interlinked field lines to reconnect as soon as they are allowed to, i.e., once they are marginally in the reconnection-allowed regime. Thus, one would expect the post-pileup $\Delta\beta$ and θ values to lie close to (and just above) the marginal $\Delta\beta = 2 \tan(\theta/2)$ condition. However, that is not seen in the data, as many of the post-pileup $\Delta\beta$ and θ are positioned well into the reconnection-allowed regime (Figure 3(a)). The fact that the post-pileup $\Delta\beta$ and θ lie away from the marginal $\Delta\beta$ - θ condition (even for $L/d_i = 0.5$) cannot be attributed to the uncertainties in the determination of the values of the post-pileup $\Delta\beta$ and θ , because the post-pileup locations, i.e., the two edges of the current sheets, are generally well defined, so the errors would be small.

(2) The presence of seven events that had the $\Delta\beta$ and θ values already in the reconnection-allowed regime pre-pileup suggests that for these events, the diamagnetic drift suppression condition was not a factor in preventing reconnection prior to field pileup, and the B_L pileup must have been caused by other factors.

We propose the following possible scenarios that could apply to both puzzles:

(1) Reconnection could have been suppressed initially if, for example, the current sheet was too thick (e.g., Sanny et al. 1994; Runov et al. 2008) or velocity shears were too large (e.g., Cassak & Otto 2011), even if the $\Delta\beta$ - θ condition allowed reconnection to occur. If such factors prevented reconnection, the magnetic flux would still pile up until all necessary conditions for reconnection were satisfied. This could be similar to the recent findings that a large number of current sheets in the solar wind do not reconnect, even though their $\Delta\beta$ and θ values are in the reconnection-allowed regime (Phan et al. 2020; Vasko et al. 2021). Thus, a current sheet could move into the reconnection-allowed regime of Equation (1), but flux would pile up until the current sheet satisfies all other conditions before reconnection could begin. MMS would cross some current sheets well in the reconnection-allowed zone. Similarly, even if reconnection was allowed pre-pileup (by Equation (1)) for the seven events, reconnection would not begin until all other conditions are met, so MMS would observe some interlinked structures pre-pileup that are in the reconnection-allowed zone yet not reconnecting.

(2) Reconnection could have occurred initially, but it was strongly driven. In the strongly driven regime, the converging (and inflowing) plasma speed may have exceeded the rate of reconnection in the interface current sheet, leading to magnetic flux pileup that enhanced the inflow Alfvén speed and thus the (dimensional) reconnection rate (Anderson et al. 1997). Thus, MMS would observe reconnecting current sheets far into the reconnection-allowed regime with flux continuing to pile up even after reconnection has begun, until the inflow Alfvén speed, and thus the reconnection rate, sufficiently increases to balance the incoming flux. Moreover, some events could start in the reconnection-allowed regime pre-pileup with

reconnection beginning, but MMS could observe strongly driven reconnection and continued pileup.

In conclusion, the comparison between pre- and post-pileup conditions suggests that in most interlinked reconnection events, field pileup in the inflow regions could be related to the diamagnetic drift suppression condition. However, there are open questions about this scenario concerning why reconnection is not triggered as soon as the boundary conditions of the interlinked current sheet are at the marginal state of the diamagnetic suppression condition. Also, the role of additional factors that could limit reconnection and lead to magnetic field pileup should be investigated further. Future 3D reconnection simulations should be able to shed light on these issues.

We are grateful for the dedicated efforts of the entire MMS team. This research was supported by NASA grants 80NSSC20K1781, 80NSSC18K1380, and NASA contract NNG04EB99C. The data are available at the MMS Science Data Center at lasp.colorado.edu/mms/sdc/public/.

ORCID iDs

K. Maheshwari  <https://orcid.org/0000-0003-1198-4685>
 T. D. Phan  <https://orcid.org/0000-0002-6924-9408>
 M. Øieroset  <https://orcid.org/0000-0003-3112-1561>
 N. Fargette  <https://orcid.org/0000-0001-6308-1715>
 B. Lavraud  <https://orcid.org/0000-0001-6807-8494>
 J. L. Burch  <https://orcid.org/0000-0003-0452-8403>
 R. J. Strangeway  <https://orcid.org/0000-0001-9839-1828>
 D. J. Gershman  <https://orcid.org/0000-0003-1304-4769>
 B. L. Giles  <https://orcid.org/0000-0001-8054-825X>

References

- Anderson, B. J., Phan, T. D., & Fuselier, S. A. 1997, *JGR*, **102**, A5
 Cassak, P. A., & Otto, A. 2011, *PhPI*, **18**, 074501
 Fargette, N., Lavraud, B., Øieroset, M., et al. 2020, *GeoRL*, **47**, e87626
 Fargette, N., Lavraud, B., Rouillard, A., et al. 2021, *A&A*, **650**, A11
 Gosling, J. T., & Phan, T. D. 2013, *ApJL*, **763**, L39
 Kacem, I., Jacquy, C., Génot, V., et al. 2018, *JGRA*, **123**, 1779
 Øieroset, M., Phan, T. D., Drake, J. F., et al. 2019, *GeoRL*, **46**, 1937
 Øieroset, M., Phan, T. D., Haggerty, C., et al. 2016, *GeoRL*, **43**, 5536
 Paschmann, G., Baumjohann, W., Scokpe, N., Phan, T.-D., & Luhr, H. 1993, *JGR*, **98**, 13409
 Paschmann, G., Øieroset, M., & Phan, T. D. 2013, *SSRv*, **178**, 385
 Phan, T. D., Bale, S. D., Eastwood, J. P., et al. 2020, *ApJS*, **246**, 34
 Phan, T. D., Gosling, J. T., Paschmann, G., et al. 2010, *ApJL*, **719**, L199
 Phan, T.-D., Paschmann, G., Baumjohann, W., Scokpe, N., Luhr, H., et al. 1994, *JGR*, **99**, 121
 Phan, T. D., Paschmann, G., Gosling, J. T., et al. 2013, *GeoRL*, **40**, 11
 Pollock, C., Moore, T., Jacques, A., et al. 2016, *SSRv*, **199**, 331
 Qi, Y., Russell, C. T., Jia, Y.-D., & Hubbert, M. 2020, *GeoRL*, **47**, e90314
 Runov, A., Baumjohann, W., Nakamura, R., et al. 2008, *JGRA*, **113**, A07S27
 Russell, C. T., Anderson, B. J., Baumjohann, W., et al. 2014, *SSRv*, **199**, 189
 Russell, C. T., & Qi, Y. 2020, *GeoRL*, **47**, e87620
 Sanny, J., McPherron, R. L., Russell, C. T., et al. 1994, *JGR*, **99**, 5805
 Sonnerup, B. U. Ö., & Cahill, L. J., Jr. 1967, *JGR*, **72**, 171
 Swisdak, M., Opher, M., Drake, J. F., & Alouani, B. F. 2010, *ApJ*, **710**, 1769
 Swisdak, M., Rogers, B. N., Drake, J. F., & Shay, M. A. 2003, *JGRA*, **108**, 1218
 Vasko, I. Y., Alimov, K., Phan, T. D., et al. 2021, *ApJL*, **923**, L19
 Yamada, M. 2010, *RvMP*, **82**, 603